View metadata, citation and similar papers at core.ac.uk

brought to you by CORE

provided by Diposit Digital de Documents de la UAB

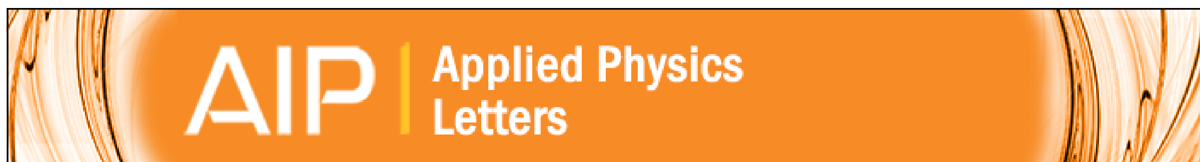

Formation of Pd2Si on single-crystalline Si (100) at ultrafast heating rates: An in-situ analysis by nanocalorimetry

M. Molina-Ruiz, A. F. Lopeandía, M. González-Silveira, Y. Anahory, M. Guihard, G. Garcia, M. T. Clavaguera-Mora, F. Schiettekatte, and J. Rodríguez-Viejo

Citation: Applied Physics Letters **102**, 143111 (2013); doi: 10.1063/1.4800934
View online: http://dx.doi.org/10.1063/1.4800934
View Table of Contents: http://scitation.aip.org/content/aip/journal/apl/102/14?ver=pdfcov
Published by the AIP Publishing

Re-register for Table of Content Alerts

Create a profile.
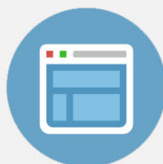
Sign up today!

This article is copyrighted as indicated in the article. Reuse of AIP content is subject to the terms at: http://scitation.aip.org/termsconditions. Downloaded to IP: 158.109.223.71 On: Mon, 17 Feb 2014 15:06:23

Formation of Pd_2Si on single-crystalline Si (100) at ultrafast heating rates: An *in-situ* analysis by nanocalorimetry

M. Molina-Ruiz,[1] A. F. Lopeandía,[1] M. González-Silveira,[1] Y. Anahory,[2] M. Guihard,[2] G. Garcia,[1] M. T. Clavaguera-Mora,[1] F. Schiettekatte,[2] and J. Rodríguez-Viejo[1,3]
[1]*Grup de Nanomaterials i Microsistemes, Departament de Física, Universitat Autònoma de Barcelona, 08193 Bellaterra, Spain*
[2]*Regroupement québécois sur les materiaux de pointe, Université de Montréal, P.O. Box 6128, Station Centre-Ville, Montréal, Québec H3C 3J7, Canada*
[3]*MATGAS Research Centre, UAB Campus, 08193 Bellaterra, Spain*

(Received 1 February 2013; accepted 25 March 2013; published online 10 April 2013)

The kinetics of intermediate phase formation between ultrathin films of Pd (12 nm) and single-crystalline Si (100) is monitored by *in-situ* nanocalorimetry at ultrafast heating rates. The heat capacity curves show an exothermic peak related to the formation of Pd_2Si. A kinetic model which goes beyond the conventional linear-parabolic growth to consider independent nucleation and lateral growth of Pd_2Si along the interface and vertical growth mechanisms is developed to fit the calorimetric curves. The model is used to extract the effective interfacial nucleation/growth and diffusion coefficients at the unusually high temperatures of silicide formation achieved at very fast heating rates. © *2013 American Institute of Physics*. [http://dx.doi.org/10.1063/1.4800934]

The fabrication of nm-size transistors in complementary metal-oxide-semiconductor (CMOS) technology highly depends on the formation of low-ohmic contacts by the reaction between silicon and a thin metallic layer. As the dimensions of the devices are reduced to the nm scale, the thermally induced solid-state formation of the silicide phase becomes extremely dependent on process parameters and material characteristics, such as metal thickness, substrate orientation, or surface roughness.[1–3] The reaction has often been analyzed by *in-situ* X-ray diffraction (XRD) to monitor sequential phase formation during a temperature excursion or isothermal measurements. At faster heating rates, synchrotron radiation offers a promising route to *in-situ* characterize the silicide reaction[4,5] and can be combined with electrical or optical measurements to obtain complementary information on the reaction. A suitable method to access the thermodynamic and kinetic parameters of a reaction is differential scanning calorimetry (DSC).[6] It has been previously used to characterize reactions in thin multilayer systems[7,8] and also amorphous and polycrystalline thick layers on substrates.[9] Recently, a study of Pd_2Si formation between 50 nm thick films of Pd with a thin monocrystalline Si substrate was carried out by conventional DSC at heating rates ranging from 25 to 100 K/min.[10] However, techniques such as rapid thermal annealing (RTA) (heating rates, $\beta \sim 100$ K/s) or pulsed laser annealing (PLA) ($\beta \sim 10^6$–10^7 K/s) are gaining widespread use in nm-scale devices because of their superior control in the activation and localization of dopants.[11] PLA is also being tested for Si-rich silicide formation[12] because of the reduced thermal budget relative to those of conventional furnace annealing approaches. The use of very thin films and faster heating ramps in silicide formation can modify the temperature of the reaction and may, as well, introduce changes in the physical-chemical mechanisms that control the development of the intermediate phases. Therefore, it is questionable if conventional DSC studies on thick films at close to 0.67 K/s may be informative enough of reaction processes occurring at the much higher heating rates relevant for nm-size chip contacts. As a consequence, it is relevant to check if different factors control the kinetics in fast thermal processing. Extension of previous studies to analyze intermediate phase sequence and formation at higher heating rates to mimic real processing will thus provide a better understanding about the phase formation by reactive diffusion in thin films and devices.[13] Only recently, first measurements by fast scanning nanocalorimetry on Ni/amorphous Si thin films at heating rates of 10^5 K/s have been reported,[14] but no comparable data exist yet on the more interesting reaction between an ultrathin metal layer and monocrystalline Si at such fast heating rates. We report an *in-situ* study of silicide formation at ultrafast heating rates, spanning 3–10 $\times$ 10^4 K/s, between a metal, in this case Pd, and monocrystalline Si. We use Pd-Si as a model system since only one stable phase, hexagonal Pd_2Si, forms below 700 °C. In addition, we show that nanocalorimetric data can be fitted with a model that includes independent interfacial nucleation/lateral growth and vertical growth processes to extract the most relevant kinetic parameters.

Thin film nanocalorimetric sensors with a sensitive area made of single-crystalline Si (100) were microfabricated starting from silicon on insulator wafers following a procedure described elsewhere.[15] The calorimetric chips were mounted on a custom made probe in differential configuration.[16] The native oxide covering the surface of the 300 nm thick Si (100) single crystal was etched with a 5% diluted HF solution to obtain an H-terminated Si surface. A self-aligned shadow mask was used to deposit the Pd film on the sensitive area of the sensor. Pd was grown from pure Pd pellets (99.95% purity) at room temperature by electron beam evaporation in a Leybold UNIVEX 450 high vacuum chamber. The Pd thickness was estimated with a quartz crystal monitor located nearby the calorimetric cells. Nanocalorimetric measurements were carried out *in-situ* at a base pressure of 2×10^{-6} mbar and therefore heat losses due

 © 2013 American Institute of Physics

This article is copyrighted as indicated in the article. Reuse of AIP content is subject to the terms at: http://scitation.aip.org/termsconditions. Downloaded to IP: 158.109.223.71 On: Mon, 17 Feb 2014 15:06:23

to convection and conduction through the atmosphere can be neglected.[17]

The nanocalorimetric measurements consisted of the following consecutive steps: (a) 100 successive scans up to temperatures around 850 K to obtain the initial offset in heat capacity between the empty calorimetric cells (baseline correction), (b) Deposition of 12 ± 1 nm thick Pd films at a rate of 0.10 ± 0.01 nm/s, (c) Annealing of the Pd layer at 375 K for 15 min, (d) Calorimetric scan up to 850 K to complete the Pd-Si reaction, and (e) 100 consecutive temperature scans after the silicide reaction is completed. The second, post-reaction, scan is used for baseline subtraction in order to obtain accurate data to model the calorimetric traces. Several heating rates were used in step (d) to extract kinetic information of the intermetallic reaction on different samples of identical thickness. Since the reaction is irreversible, the averaging of multiple scans, widely used in fast scanning nanocalorimetry to improve the signal-to-noise ratio, is not useful and the first scan after Pd deposition contains all the valuable information of the silicide reaction. The noise in the heat capacity in the single scans is around 0.4 nJ/K at 300 K. The temperature calibration was independently determined afterwards on every chip by measuring the melting point of Sn and Al layers, grown on top of the Pd_2Si after capping by a thin insulating film. Cross sectional transmission electron microscopy (XTEM, Jeol JEM-2011 at 200 kV), field emission scanning electron microscopy (FESEM, Carl Zeiss Merlin, operated at 1 kV), and micro X-ray diffraction (μXRD, Bruker D-8 Advance system coupled with a Gadds detector with Cu Kα, $\lambda = 1.5418$ Å) were used to characterize the final product of the transformation after thermal ramping.

Figure 1 shows the calorimetric experimental data for a sample measured at 3×10^4 K/s. The onset of the silicide reaction occurs at ~9 ms, where a large variation of the slope in the differential voltage signal is observed. The growth of the Pd layer slightly delays the temperature of the sample calorimetric cell with respect to the empty reference cell up to the onset of the reaction (Fig. 1(b) and inset). The acceleration in the temperature evolution is more clearly identified in Fig. 1(c) that shows the increase of the heating rate as a consequence of the exothermic reaction in the sample during the first scan (red curve). Finally, the specific heat capacity is obtained by applying corrections due to different addenda and heating rates (β) between the sample and the reference cell (Fig. 1(d)). It is clearly observed that the Pd_2Si is completely formed before 730 K during the first pulse and no more exothermic reactions are observed on successive scans.

The subtraction of the 1st and 2nd scans for the three heating rates results in the calorimetric traces shown in Fig. 2(a). Integration of the exothermic peaks yields an enthalpy of formation $\Delta H_f = 260 \pm 20$ J/g in agreement with previously reported values 260.2 ± 10.1 J/g (Ref. 19) and 259.0 ± 9.7 J/g (Ref. 20) for Pd_2Si formation. Similar agreement was found in the analysis of the reaction between Ni and a-Si by fast-scanning calorimetry and DSC.[13,14] Our result do not exclude, however, that thinner films may have variations in the enthalpy of formation due to size effects. On the other hand, the Kissinger analysis indicates an apparent activation energy $E_{ap} = 0.40 \pm 0.05$ eV greatly differing from the activation energy of ~0.8 eV extracted from the

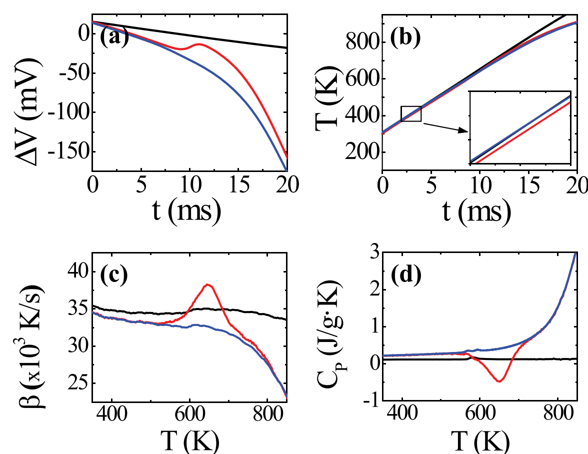

FIG. 1. Calorimetric data obtained during an up scan at a heating ramp at $\sim 3 \times 10^4$ K/s till 850 K. Black curve: difference between empty calorimeters; red curve: difference between sample (1st scan) and reference; blue curve: difference between sample (2nd scan) and reference cell. (a) Voltage difference as a function of time. (b) Temperature of the sample calorimetric cell versus annealing time. (c) Heating rate (β) vs. temperature during calorimetric scans. (d) Specific heat capacity data as a function of temperature.

DSC data of Hoummada *et al.*[10] at low heating rates (in the range 0.4–1.7 K/s) with 50 nm thick Pd layers.

To gain more insight into the specific thermodynamic processes playing a role in the formation of the silicide and their activation energies we carry out a detailed simulation of our calorimetric data. Our first attempt consists of fitting the experimental data shown in Fig. 2 using a linear-parabolic model to match calorimetric traces measured at slower heating rates.[10] However, the abrupt onset of the peaks in Fig. 2(a) could only be obtained by introducing the nucleation of the silicide phase. The differences between both models can be appreciated in Fig. 2(b). The proposed model considers the formation of a single phase, Pd_2Si, following two main processes: nucleation and lateral growth of Pd_2Si along the initial interface and vertical growth of the silicide phase. Its main features have been previously described in other systems.[8,21,22] Briefly, the fraction of

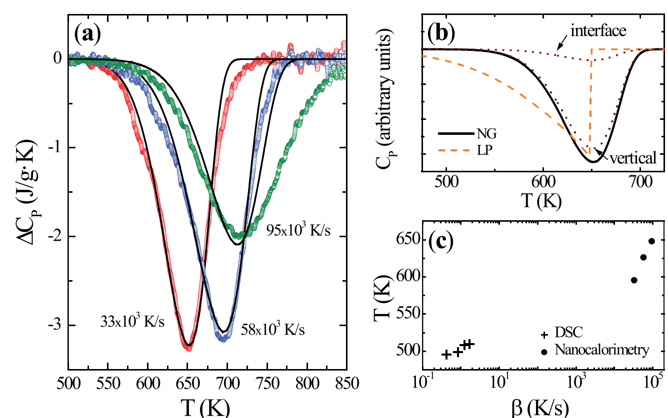

FIG. 2. (a) Specific heat capacity difference between 1st and 2nd scan vs. Temperature for 12 nm Pd samples measured at three different rates. The continuous lines correspond to the calculated data using the nucleation and growth model. (b) Comparison between linear-parabolic growth (LP) and nucleation and growth models (NG) (see supplementary material for further details).[18] The dotted lines within the NG peak are the interface and vertical contribution to the calorimetric peak. (c) T-HR-T diagram for the Pd_2Si formation compared with DSC data from Ref. 10.

This article is copyrighted as indicated in the article. Reuse of AIP content is subject to the terms at: http://scitation.aip.org/termsconditions. Downloaded to IP: 158.109.223.71 On: Mon, 17 Feb 2014 15:06:23

silicide phase that is formed at the Pd/Si interface can be written within the Johnson–Mehl–Avrami–Kolmogorov model as (see supplementary material)[18]

$$x_L(T) = 1 - \exp(-x_L^{ext}(T)), \quad \text{where}$$
$$x_L^{ext}(T) = \pi \int_{T_0}^{T} \frac{I(T')}{\beta(T')} \left\{ \int_{T'}^{T} \frac{U_L(T'')}{\beta(T'')} dT'' \right\}^2 dT', \qquad (1)$$

where both the nucleation rate, I, and the lateral growth rate, U_L, have an Arrhenius temperature dependence, β is the heating rate which is temperature dependent, and the initial nuclei have been assumed to be cylinders with negligible radius r_o and height L_o. The vertical growth of the new phase can be either reaction or diffusion controlled, following the growth laws, $L^2 \propto Dt \;\; or \;\; L \propto Kt$, respectively, where L is the thickness of the Pd_2Si film, D is an effective diffusion coefficient that does not discriminate in which direction is the new film growing (i.e., consuming Pd or Si) and K is the interfacial reaction constant. The ΔC_P can be calculated as the temperature derivative of the total transformed fraction, x, multiplied by the reaction enthalpy, ΔH, $\Delta Cp(T) = \Delta H \frac{dx}{dT}$. The calculation is performed in a discrete way for every nucleus. When a certain fraction of Pd_2Si has vertically grown enough to reach the final thickness of the silicide layer, L_f, it stops growing. This approximation produces a smooth ending of the calorimetric peaks provided the nucleation/lateral growth along the interface remains the limiting mechanism. The presence of a single peak is related to the significant overlap between the interfacial nucleation and growth and the vertical growth (Fig. 2(b)). The model reproduces satisfactorily the calorimetric traces measured at heating rates 33×10^3 K/s and 58×10^3 K/s, but fails to explain the curve width measured at 95×10^3 K/s. The best fit for the experimental data have been obtained using the values shown in Table I (see supplementary material).

The activation energy obtained from the Kissinger method, 0.4 eV/at, is compatible with the apparent activation energy for the reaction at the interface, E_A. Therefore, our model suggests that the thermodynamic processes controlling the formation of Pd_2Si at the very fast rates used in this work are related to the nucleation and lateral growth during the initial stages of growth. The results of our fast scanning nanocalorimetry experiments and those already reported by conventional DSC are summarized in the temperature-heating rate-transformation (T-HR-T) diagram shown in Fig. 2(c). In this T-HR-T diagram, the temperature needed to achieve ∼10% volume fraction of Pd_2Si (or ∼2.2 nm thick Pd_2Si) is plotted as a function of the heating rate. To fit the data from Ref. 10, an initial interlayer of palladium silicide of thickness 4 nm had to be added to the model in accordance with the finding that sputtered Pd films on Si form an intermediate layer during the deposition process.[23] These data highlight the difference in the transformation mechanism observed between conventional DSC on sputtered Pd layers and fast-scanning nanocalorimetry on Pd films grown by electron beam evaporation at room temperature. The change in the activation energies could originate from a true change of mechanism induced by the large variations in heating rate or from differences in the initial surface state of the Si wafer. The formation of a thin SiO_2 layer on the Si surface during the initial measurement protocol (baseline determination) may inhibit the initial reaction at almost room temperature between Pd and Si, retarding the nucleation of the new phase and, enhancing the overlap of the calorimetric traces associated to the nucleation and growth and the vertical growth of the silicide phase as shown in Fig. 2(b). XTEM observations have not revealed the presence of the oxide at the interface between Pd_2Si and Si, however, we do not rule out the possibility of an oxide mediated formation of the silicide phase, as has been observed in other investigations.[24,25]

The FESEM image shown in Fig. 3(a) corresponds to the surface of a sample heated up to 850 K at 33×10^3 K/s. The surface is smooth and contains microcracks oriented parallel to the Si (001) planes. The presence of cracks at the surface may be related to built-in stresses during the silicide growth. When the sample is cycled many times (Figure 3(b)), the microstructure dramatically changes by generating a high density of protrusions and increasing the roughness of the surface. The images obtained using the backscattered electrons (BSE) show that substantial cycling introduces inhomogeneities in composition which correspond to areas with different Pd-Si ratios (inset of Figure 3(b)). The agglomeration of Pd_2Si is well documented for isothermal reaction studies of Pd on Si (001).[26] Our results show that fast heating reduces Si segregation and yields smother films which may be advantageous for chip interconnections. The XTEM images (shown in SM) confirm the roughness of the samples after substantial cycling. Electron diffraction (ED) performed on film section (Fig. 3(c), inset) corroborates the formation of the Pd_2Si hexagonal structure (PDF 00-019-0893). No evidence of free palladium is detected. ED with almost discrete spots indicates a preferred orientation of the grains. The XRD pattern (Fig. 3(c)) confirmed the preferred orientation of the Pd_2Si layer along the [00*l*] direction, as 008 reflection peak presents a larger intensity than that expected when compared with the powder diffraction pattern. Also, no reflections corresponding to the palladium were observed, confirming the consumption of the whole Pd layer during the process.

In conclusion, we have performed *in-situ* nanocalorimetric experiments and measured the heat capacity during the reaction between 12 nm Pd thin films and single-crystalline Si (100) at ultrafast heating rates. The enthalpy of the reaction is consistent with values reported at slower heating rates for the formation of Pd_2Si, the only phase observed in XTEM and μXRD analysis of the samples. By modeling the calorimetric signal, we determined the kinetics of the

TABLE I. Values used for the modeling of the calorimetric signal. Uncertainties are estimated from the tolerance to produce comparable chi^2 in the fit.

$(IU_L^2)^{1/3} = A_o \exp(-E_A/k_BT)$	
A_o	$(4.0 \pm 0.5) \times 10^5$ nuclei/s
E_A	(0.38 ± 0.04) eV
$D = D_o \exp(-E_D/k_BT)$	
D_o	(0.05 ± 0.04) cm^2/s
E_D	(1.00 ± 0.20) eV
L_o, L_f	2 ± 1 nm, 20 ± 1 nm

This article is copyrighted as indicated in the article. Reuse of AIP content is subject to the terms at: http://scitation.aip.org/termsconditions. Downloaded to IP: 158.109.223.71 On: Mon, 17 Feb 2014 15:06:23

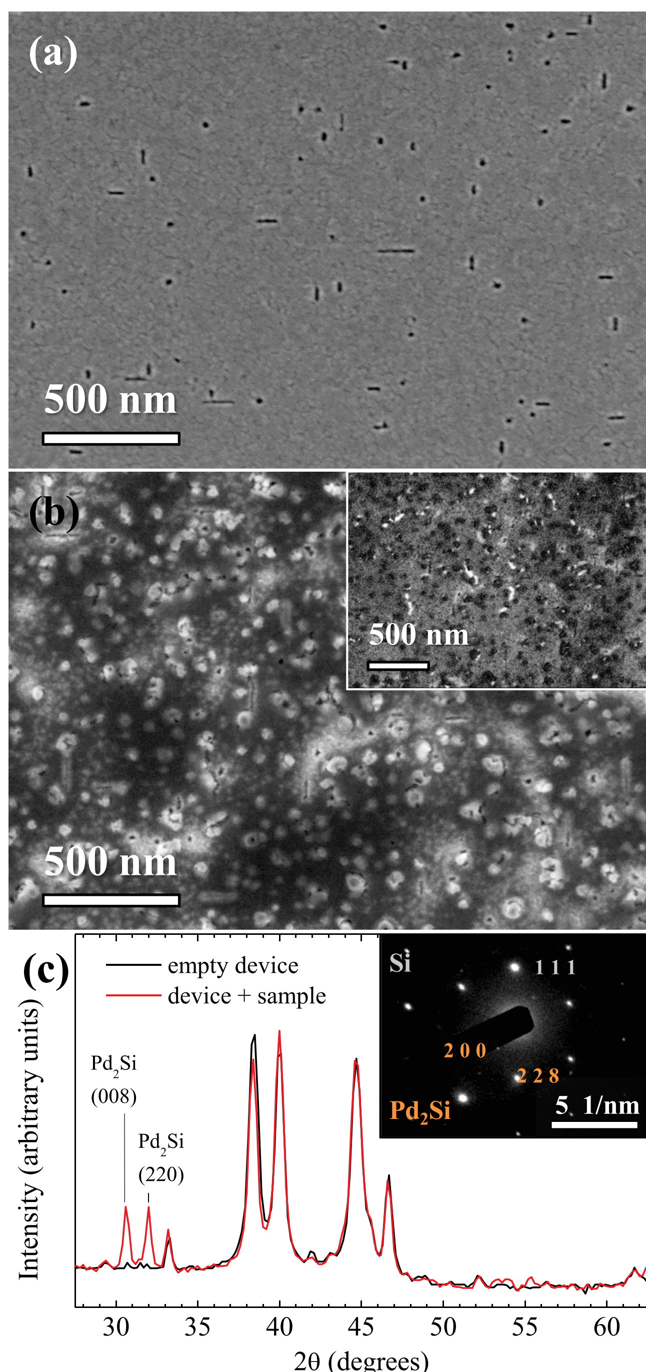

FIG. 3. (a) FESEM image of a sample fast ramped up to 850 K. (b) FESEM image of a sample after multiple fast scans to 850 K. Inset: BSE image showing compositional inhomogeneities. (c) μXRD pattern of sample shown in (b), the pattern of the empty nanocalorimeter is shown for comparison. Inset: ED pattern; orange reflections correspond to Pd_2Si sample, grey reflections to Si (100) substrate.

reaction is limited by the nucleation and lateral growth along the Pd/Si interface.

Researchers from GNaM acknowledge financial support from Generalitat de Catalunya and Ministerio de Economía y Competitividad through Grants SGR2009-01225 and MAT2010-15225, respectively, and from Marie Curie European Reintegration Grant within the 7th European Community Framework Programme. Researchers from RQMP acknowledge funding from FQRNT and NRSEC. The authors acknowledge the Cornell Nanofabrication Facility and the Laboratoire de nanofabrication of the École Polytechnique de Montreal for chip microfabrication, as well as the Servei de Microscòpia from the Universitat Autònoma de Barcelona for sample preparation and microscopy images.

[1]R. W. Bower, D. Sigurd, and R. E. Scott, Solid-State Electron. **16**(12), 1461–1471 (1973).
[2]W. D. Buckley and S. C. Moss, Solid-State Electron. **15**(12), 1331 (1972).
[3]G. Y. Robinson, Appl. Phys. Lett. **25**(3), 158–160 (1974).
[4]S. Gaudet, P. Desjardins, and C. Lavoie, J. Appl. Phys. **110**(11), 113524 (2011).
[5]J. Fouet, M. I. Richard, C. Mocuta, C. Guichet, and O. Thomas, Nucl. Instrum. Methods B **284**, 74–77 (2012).
[6]M. T. Clavaguera-Mora, N. Clavaguera, D. Crespo, and T. Pradell, Prog. Mater. Sci. **47**(6), 559–619 (2002).
[7]E. Ma, C. V. Thompson, and L. A. Clevenger, J. Appl. Phys. **69**(4), 2211–2218 (1991).
[8]M. Gonzalez-Silveira, M. T. Clavaguera-Mora, F. Pi, and J. Rodríguez-Viejo, Phys. Rev. B **69**(11), 113411 (2004).
[9]C. Michaelsen, K. Barmak, and T. P. Weihs, J. Phys. D-Appl. Phys. **30**(23), 3167–3186 (1997).
[10]K. Hoummada, A. Portavoce, C. Perrin-Pellegrino, D. Mangelinck, and C. Bergman, Appl. Phys. Lett. **92**(13), 133109 (2008).
[11]H.-Y. Chen, C.-Y. Lin, M.-C. Chen, C.-C. Huang, and C.-H. Chien, J. Electrochem. Soc. **158**(8), H840–H845 (2011).
[12]H.-Y. Chen, C.-Y. Lin, C.-C. Huang, C.-H. Chien, Microelectron. Eng. **87**(12), 2540–2543 (2010).
[13]L. P. Cook, R. E. Cavicchi, N. Bassim, S. Eustis, W. Wong-Ng, I. Levin, U. R. Kattner, C. E. Campbell, C. B. Montgomery, W. F. Egelhoff, and M. D. Vaudin, J. Appl. Phys. **106**(10), 104909 (2009).
[14]Ravi K. Kummamuru, L. de la Rama, L. Hu, M. D. Vaudin, M. Y. Efremov, M. L. Green, D. A. LaVan, and L. H. Allen, Appl. Phys. Lett. **95**(18), 181911 (2009).
[15]Y. Anahory, M. Guihard, D.Smeets, R. Karmouch, F. Schiettekatte, P. Vasseur, P. Desjardins, L. Hu, L. H. Allen, E. Leon-Gutierrez, and J. Rodriguez-Viejo, Thermochim. Acta **510**(1–2), 126–136 (2010).
[16]M. Molina-Ruiz, A. F. Lopeandia, F. Pi, D. Givord, D. O. Bourgeois, and J. Rodriguez-Viejo, Phys. Rev. B **83**(14), 140407 (2011).
[17]A. F. Lopeandía, J. Rodríguez-Viejo, M. Chacon, M. T. Clavaguera-Mora, and F. J. Munoz, J. Micromech. Microeng. **16**(5), 965–971 (2006).
[18]See supplementary material at http://dx.doi.org/10.1063/1.4800934 for more details on the calorimetric modeling.
[19]F. R. Boer, R. Boom, W. C. M. Mattens, A. R. Miedema, and A. K. Niessen, in *Cohesion in Metals: Transition Metal Alloys* (North Holland, 1988).
[20]S. V. Meshel and O. J. Kleppa, J. Alloys Compd. **274**(1–2), 193–200 (1998).
[21]K. R. Coffey, L. A. Clevenger, K. Barmak, D. A. Rudman, and C. V. Thompson, Appl. Phys. Lett. **55**(9), 852–854 (1989).
[22]M. Gonzalez-Silveira, J. Rodriguez-Viejo, G. Garcia, G. F. Pi, F. J. Ager, J. L. Labar, A. Barna, M. Menyhard, and L. Kotis, J. Appl. Phys. **100**(11), 113522 (2006).
[23]T. Hosoi, K. Sano, K. Hosawa, and K. Shibahara, Jpn. J. Appl. Phys. **46**(4B), 1929–1933 (2007).
[24]C. Detavernier, R. L. Van Meirhaeghe, F. Cardon, R. A. Donaton, and K. Maex, Appl. Phys. Lett. **74**(20), 2930–2932 (1999).
[25]R. T. Tung, Appl. Phys. Lett. **68**(24), 3461–3463 (1996).
[26]R. Suryana, O. Nakatsuka, and S. Zaima, Jpn. J. Appl. Phys. **50**(5), 05EA09 (2011).

This article is copyrighted as indicated in the article. Reuse of AIP content is subject to the terms at: http://scitation.aip.org/termsconditions. Downloaded to IP: 158.109.223.71 On: Mon, 17 Feb 2014 15:06:23